Disappearance of Antiferromagnetic Spin Excitations in Overdoped $La_{2-x}Sr_xCuO_4$

S. Wakimoto,[1] K. Yamada,[2] J. M. Tranquada,[3] C. D. Frost,[4] R. J. Birgeneau,[5] and H. Zhang[6]

[1]*Quantum Beam Science Directorate, Japan Atomic Energy Agency, Tokai, Ibaraki 319-1195, Japan*
[2]*Institute for Materials Research, Tohoku University, Katahira, Sendai 980-8577, Japan*
[3]*Brookhaven National Laboratory, Upton, New York 11973-5000, USA*
[4]*ISIS Facility, Rutherford Appleton Laboratory, Chilton, Didcot, OX11 0QX, United Kingdom*
[5]*Department of Physics, University of California, Berkeley, Berkeley, California 94720, USA*
[6]*Department of Physics, University of Toronto, Toronto, Ontario, Canada M5S 1A7*
(Received 6 September 2006; published 11 June 2007)

Magnetic excitations for energies up to ~ 100 meV are studied for overdoped $La_{2-x}Sr_xCuO_4$ with $x = 0.25$ and 0.30, using time-of-flight neutron spectroscopy. Comparison of spectra integrated over the width of an antiferromagnetic Brillouin zone demonstrates that the magnetic scattering at intermediate energies, $20 \lesssim \omega \lesssim 100$ meV, progressively decreases with overdoping. This strongly suggests that the magnetism is not related to Fermi surface nesting, but rather is associated with a decreasing volume fraction of (probably fluctuating) antiferromagnetic bubbles.

While remarkable progress has been made over the last few years in identifying common features of the spin excitations in superconducting cuprates [1–5], there continues to be considerable controversy over the microscopic origin of these dynamic antiferromagnetic (AF) correlations. Of particular relevance are spin excitations with energies on the scale of the superconducting gap [6]. Do these dynamic correlations reflect residual local antiferromagnetism connected with the parent insulator (into which holes have been doped), or, alternatively, are they a direct result of the shape (nesting) of the electronic Fermi surface [7]? In the first case, one expects that, with sufficient doping, all vestiges of the parent insulator should disappear, especially spin fluctuations on the scale of the AF superexchange energy. This is because AF correlations are likely to survive due to charge segregation [8], and beyond some critical hole density charge segregation should become energetically unfavorable [9]. In the second case, the existence of low-energy spin fluctuations would depend only on the nesting properties of the Fermi surface, as for spin-density waves in chromium and its alloys [10]. The debate on this issue is fundamental to understanding the ''normal'' state of layered cuprates, out of which the superconductivity develops on cooling.

In this Letter, we directly test these two alternative scenarios by experimentally searching for spin fluctuations in overdoped $La_{2-x}Sr_xCuO_4$ (LSCO). One recent neutron-scattering study on overdoped LSCO [11] has revealed that the incommensurate magnetic scattering at low energy ($\omega \lesssim 10$ meV) decreases linearly with T_c as doping increases for $x \gtrsim 0.25$, and disappears coincidentally with the disappearance of the bulk superconductivity at $x = 0.30$. While that result suggests a clear correlation between the magnetic excitations and superconductivity, it leaves open the possibility that the spectral weight has shifted to higher, but still relevant, energies. To resolve this issue, we have used a time-of-flight neutron-scattering technique to

search for magnetic excitations at energies up to 100 meV in overdoped LSCO with $x = 0.25$ and 0.30. To achieve good sensitivity, we integrate the measured scattering over wide momentum and energy intervals, and compare the results with data for $La_{1.875}Ba_{0.125}CuO_4$ (LBCO 1/8) [12]. For $x = 0.25$, we find that the magnetic scattering in the intermediate energy range $20 \lesssim \omega \lesssim 100$ meV is reduced by a factor of 2. The nonsuperconducting $x = 0.30$ sample shows essentially no magnetic scattering for $\omega \lesssim 60$ meV, and only a weak signal for $\omega \gtrsim 60$ meV. Given that recent angle-resolved photoemission studies have shown that the shape of the Fermi surface becomes better matched to a nearly-AF response in the overdoped regime [13,14], opposite to the observed trend in magnetic signal strength, the present results provide compelling evidence that electron-hole excitations do not provide the dominant contribution to the magnetic response in superconducting cuprates.

Single crystals of LSCO with $x = 0.25$ and 0.30 were prepared by the traveling-solvent floating-zone method, in the same manner as for the crystals used for the previous triple-axis measurements [11]. After growth, the crystals were annealed in an oxygen atmosphere to minimize any oxygen vacancies. From magnetization measurements, the $x = 0.25$ crystals have $T_c \sim 14$ K, while the $x = 0.30$ samples show no sign of bulk superconductivity down to 2 K, consistent with the results of Tanabe *et al.* [15]. The crystal structures of both compositions have tetragonal ($I4/mmm$) symmetry, with lattice constants of $a = b = 3.76$ Å at 10 K. For convenience, we will use the notation corresponding to the orthorhombic unit cell relevant to LSCO at lower doping. In this notation, the a and b axes are parallel to the diagonal Cu-Cu directions of the CuO_2 square lattice and, therefore, the reciprocal lattice unit (r.l.u.) corresponds to 1.18 Å^{-1}. The orientation of the low-energy incommensurate peaks around the AF wave vector $\mathbf{Q}_{AF} = (1, 0)$ is indicated at the top of Fig. 2.

Neutron-scattering experiments were carried out at the MAPS time-of-flight spectrometer installed at the ISIS pulsed neutron source, UK. For each composition, eight crystal rods with a total volume of ~ 9.5 cm^3 were coaligned and oriented such that the [001] axis was parallel to the incident beam. Measurements were performed either with an incident energy $E_i = 80$ meV and chopper frequency $f_{ch} = 300$ Hz or with $E_i = 140$ meV and $f_{ch} = 400$ Hz. These cross sections are put on an absolute scale by taking account of the sample volume and normalizing to the signal from a standard vanadium foil. Data have been analyzed after summing up intensities of detectors that cover symmetric positions in the (HK) zone to gain counting statistics.

The challenge in analyzing the data is to identify the magnetic signal in the overdoped samples. Figures 1(a) and 1(b) show intensity maps of scattering cross sections for LSCO $x = 0.25$ and LBCO $1/8$ (from Xu *et al.* [12]), respectively, that are integrated over the q range of $0.5 \leq H \leq 1.5$ r.l.u. and then multiplied by the energy transfer ω. (Data for $x = 0.30$ are not shown here as they are virtually indistinguishable from $x = 0.25$ in this format [16].) The integration over a wide band in H is done to sum up magnetic signal that might be spread over a significant range in **Q**. The multiplication by ω is intended to compensate for the energy dependence of the scattering signals; this approach has been used previously to display the spin-wave dispersion in stripe-ordered La$_{1.67}$Sr$_{0.33}$NiO$_4$ [17]. In the latter case, the magnetic signal is comparable to the phonon cross section. In the present case, one can detect for LBCO in Fig. 1(b) a vertical streak of magnetic signal centered around **Q**$_{AF}$ ($K = 0$) superimposed on a much stronger signal from phonons. In contrast, for LSCO $x = 0.25$ in Fig. 1(a), the signal is entirely dominated by the phonons. In Figs. 1(c) and 1(d), we have reduced most of the phonon contribution by subtracting the data for LSCO $x = 0.30$. (Here and in Fig. 2 the LBCO intensities have been scaled by 0.93 so that the average phonon contribution is equal to that in the LSCO samples.) These figures show qualitatively that the magnetic scattering that is concentrated near **Q**$_{AF}$ in LBCO $1/8$ has decreased significantly in LSCO $x = 0.25$, making quantitative analysis difficult.

We have found that we can identify a finite magnetic signal by taking cuts through the data along **Q** $= (1, K)$, and integrating over energy ($\omega \pm 5$ meV) as well as H ($0.5 \leq H \leq 1.5$ r.l.u). Figure 2 shows a selection of such intensity profiles for all three samples at four different energies. (Note that for 100 meV, the H integration is limited to $0.5 \leq H \leq 1.2$ r.l.u. due to limitations in detector coverage at that energy.) We expect the phonon background to be very similar for all three samples, and we take
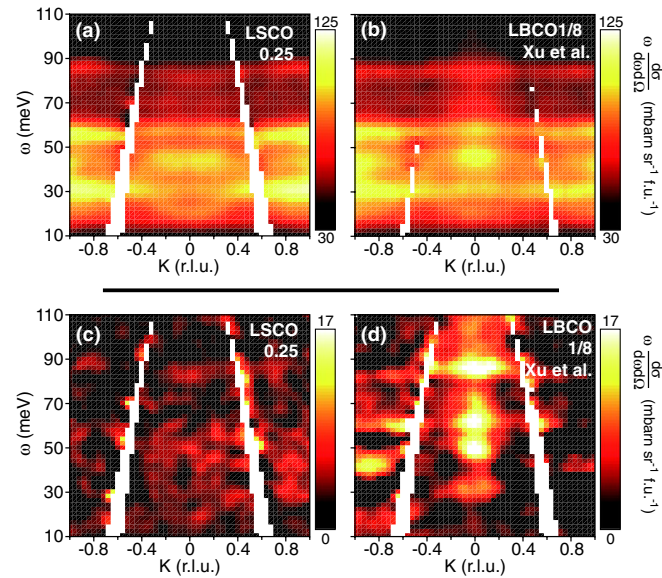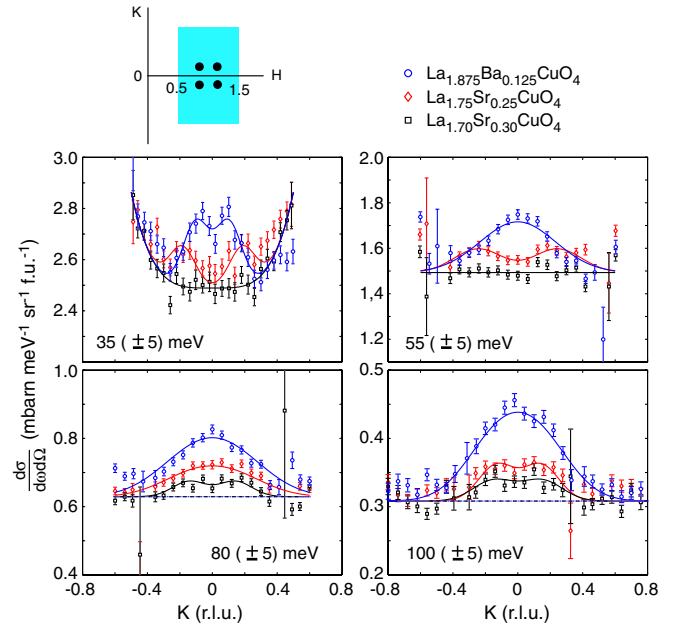

FIG. 1 (color online). Contour plots of $\omega \frac{d\sigma}{d\Omega d\omega}$ for (a) LSCO $x = 0.25$ and (b) LBCO $x = 1/8$, all measured with $E_i = 140$ meV at 10 K. Data for LBCO $x = 1/8$ are from Xu *et al.* [12]. The plotted quantities are integrated for $0.5 \leq H \leq 1.5$ r.l.u. and projected on the K axis. (c) and (d) show contour plots of differential intensities derived by subtracting data of LSCO $x = 0.30$ from those of LSCO $x = 0.25$ and those of LBCO $x = 1/8$, respectively. The white regions arising from $K \sim \pm 0.7$ correspond to areas without detector coverage.

FIG. 2 (color online). Intensity profiles cut along the K axis, with data integrated over $0.5 \leq H \leq 1.5$ r.l.u., corresponding to the H-width of the shaded area in the top figure, also integrated over an energy range of ± 5 meV about the excitation energy specified in each panel. All data are taken with $E_i = 140$ meV. Circles, diamonds, and squares represent LBCO $1/8$, LSCO $x = 0.25$ and 0.3, respectively. Solid lines are results of fits to a double-Gaussian function. The fits for $x = 0.30$ at $\omega = 35$ and 55 meV are set equal to background; in the bottom panels, background is shown by dashed lines.

it to be a constant, except at $\omega = 35$ meV, where the background has been fit to the functional form $a + bK^4$. The **Q**-dependent signal above the background is taken to be magnetic. (The maximum phonon energy is 85 meV [18], so the signal at 100 meV must be magnetic.) These profiles demonstrate a monotonic decrease in the **Q**-dependent magnetic signal with doping in the intermediate energy range, just as previously seen in the low-energy regime [11].

We are interested in evaluating the **Q**-integrated dynamic structure factor $S(\omega)$. To convert from units of the differential cross section, we make use of

$$\frac{d\sigma}{d\Omega d\omega} = \left(\frac{\gamma r_0}{2}\right)^2 \frac{k_f}{k_i} f^2(\mathbf{Q}) S(\mathbf{Q}, \omega), \quad (1)$$

where $\gamma r_0/2$ is the neutron magnetic scattering length, k_i and k_f are the wave numbers of the incident and final neutrons, respectively, and $f(\mathbf{Q})$ is the magnetic form factor. We have fit the cross-section profiles in Fig. 2 with a double Gaussian without convoluting the instrumental resolution. Since the profiles are already integrated over the relevant range in H, a simple one-dimensional integration of the fits along K is sufficient to estimate $S(\omega)$. (The same integration range was used for LBCO 1/8 in [2].) For LSCO $x = 0.30$, there is no obvious structure in the cuts at 35 and 55 meV, so we took the data to define the background.

The derived $S(\omega)$ at intermediate energies for the three samples are shown in Fig. 3 by filled symbols. Open diamonds represent results for LSCO $x = 0.25$ evaluated in a similar fashion (with a flat background) from the $E_i = $
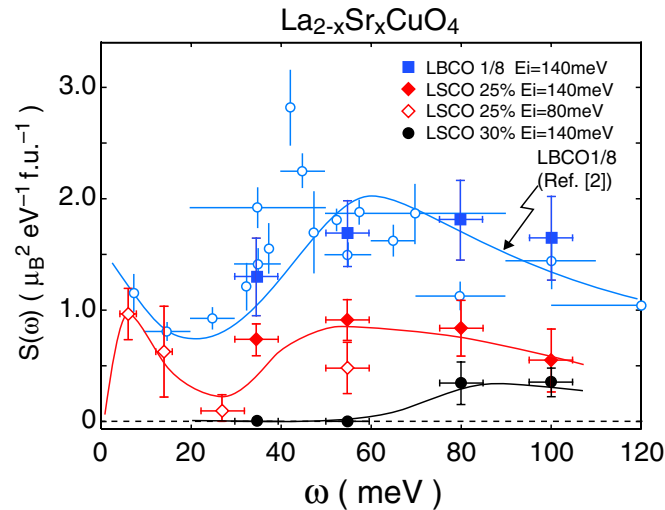
80 meV data; the better energy resolution with the smaller E_i is beneficial for evaluating the lower energy regime, $\omega < 30$ meV. The previously reported results [2] for $S(\omega)$ in LBCO 1/8 are shown by open circles in Fig. 3 as a reference. The results evaluated from the new measurements [12] for LBCO 1/8 obtained under the same conditions as for LSCO, shown by squares, are in good agreement.

To appreciate the significance of Fig. 3, we first note that the magnitude of $S(\omega)$ for LBCO 1/8 over the studied energy range is quite comparable to that recently reported for optimally doped LSCO $x = 0.16$ by Vignolle *et al.* [19]. [The results in the latter case are reported in terms of the dynamic susceptibility, $\chi(\omega)$, but that is equivalent to $S(\omega)$ at the low temperatures used in these studies.] These results are both roughly comparable to the scattering weight found in antiferromagnetic La$_2$CuO$_4$ [20]. Within this context, the decrease in magnetic signal by a factor of 2 in LSCO $x = 0.25$ is a large effect, and the further decrease for $x = 0.30$ is enormous. We are unable to identify any magnetic signal for $x = 0.30$ at energies less than 60 meV, which covers the energy scale relevant to superconductivity. The magnetic response for $x = 0.30$ is strongly depressed across an energy range characteristic of antiferromagnetic spin fluctuations.

One common theoretical approach is to attribute the magnetic susceptibility of the CuO$_2$ layers to electronic excitations across the Fermi surface [21–23]. ARPES studies have shown that the nested (flat and parallel) portions of the Fermi surface in LSCO (the ones most important for the magnetic response [24]) are enhanced for $x > 0.15$ (see Fig. 5(f) in [13]). Furthermore, the electronic dispersion in the tetragonal [110] direction is independent of doping for energies up to 70 meV [25]. Thus, if electron-hole excitations associated with nesting play an important role in the dynamic susceptibility at energies up to 70 meV, we would expect to detect a significant response in the vicinity of $\mathbf{Q}_{AF}$ in our overdoped samples. (Note that the effect of interactions, typically included through the random phase approximation, can redistribute weight in **Q** and ω but cannot create spectral weight where none would exist in a noninteracting system.) The absence of such a response in our $x = 0.30$ sample and the relative weakness of the signal for $x = 0.25$ have strongly negative implications for the significance of nesting effects. Even if we have missed a weak magnetic signal spread broadly in **Q**, that would still be distinct from the strongly **Q** dependent response expected from nesting (e.g., see Fig. 17 in [14]). We look to the theory community for a quantitative analysis of the expected electron-hole contribution in the overdoped regime.

A plausible explanation of the decrease of the total magnetic spectral weight is that the volume fraction of regions supporting magnetic correlations decreases at high doping. We have in mind that these (probably dynamic) regions are characterized by stripe correlations

FIG. 3 (color online).   **Q**-integrated dynamic structure factor $S(\omega)$ which is derived from the wide-H integrated profiles for LBCO 1/8 (squares), LSCO $x = 0.25$ (diamonds; filled for $E_i = 140$ meV, open for $E_i = 80$ meV), and $x = 0.30$ (filled circles) plotted over $S(\omega)$ for LBCO 1/8 (open circles) from [2]. The solid lines following data of LSCO $x = 0.25$ and 0.30 are guides to the eyes.

[26–28]. In the underdoped regime, the incommensurability δ increases linearly with x, consistent with a gradual increase in stripe density. The incommensurability saturates for $x \gtrsim 1/8$ [29], so that the stripe density no longer increases. A likely possibility is that, for $x > 1/8$, there is a phase separation between striped regions and more homogeneous regions.

There are independent experimental indications of phase separation in the overdoped cuprates based on muon spin rotation studies [30] and magnetization measurements [15,31]. There is also evidence from scanning tunneling microscopy on $Bi_2Sr_2CaCu_2O_{8+\delta}$ for large variations in the local magnitude of the superconducting gap [32,33]. A decrease of the superconducting volume fraction has been reported to occur in LSCO for $x \gtrsim 0.20$ [15,30,31]; note that this is considerably higher than the point $x = 1/8$, above which the CuO_2 planes cannot be uniformly stripe correlated. If one associates the superconductivity with the striped regions [34], then we speculate that the decrease of the superconducting volume fraction begins when the separation between neighboring striped regions exceeds the superconducting coherence length [35].

In conclusion, we have shown that, in overdoped LSCO, spin excitations effectively decrease with doping and disappear at $x = 0.30$ for energies typical of antiferromagnetic fluctuations. We have argued that this is strong evidence that the magnetic signal in optimally doped cuprates cannot have a dominant contribution from conventional electron-hole excitations. Instead, the antiferromagnetic spin correlations in superconducting samples must be vestiges of the parent insulator.

[1] S. M. Hayden, H. A. Mook, P. Dai, T. G. Perring, and F. Doğan, Nature (London) **429**, 531 (2004).
[2] J. M. Tranquada *et al.*, Nature (London) **429**, 534 (2004).
[3] N. B. Christensen *et al.*, Phys. Rev. Lett. **93**, 147002 (2004).
[4] C. Stock *et al.*, Phys. Rev. B **71**, 024522 (2005).
[5] D. Reznik *et al.*, Phys. Rev. Lett. **93**, 207003 (2004).
[6] H. Woo *et al.*, Nature Phys. **2**, 600 (2006).
[7] P. W. Anderson, Adv. Phys. **46**, 3 (1997).
[8] E. W. Carlson, V. J. Emery, S. A. Kivelson, and D. Orgad, in *The Physics of Superconductors*, edited by K. H. Bennemann and J. B. Ketterson (Springer-Verlag, Berlin, 2004), Vol. II.
[9] M. G. Zachar, R. Eder, E. Arrigoni, and W. Hanke, Phys. Rev. B **65**, 045109 (2002).
[10] E. Fawcett, H. L. Alberts, V. Y. Galkin, D. R. Noakes, and J. V. Yakhmi, Rev. Mod. Phys. **66**, 25 (1994).
[11] S. Wakimoto *et al.*, Phys. Rev. Lett. **92**, 217004 (2004).
[12] G. Xu, J. M. Tranquada, T. G. Perring, G. D. Gu, M. Fujita, and K. Yamada, arXiv:cond-mat/0702027.
[13] T. Yoshida *et al.*, Phys. Rev. B **74**, 224510 (2006).
[14] T. Yoshida *et al.*, J. Phys. Condens. Matter **19**, 125209 (2007).
[15] Y. Tanabe, T. Adachi, T. Noji, and Y. Koike, J. Phys. Soc. Jpn. **74**, 2893 (2005).
[16] S. Wakimoto *et al.*, Physica C (Amsterdam) (in press).
[17] H. Woo *et al.*, Phys. Rev. B **72**, 064437 (2005).
[18] L. Pintschovius, Phys. Status Solidi B **242**, 30 (2005).
[19] B. Vignolle *et al.*, Nature Phys. **3**, 163 (2007).
[20] S. M. Hayden *et al.*, Phys. Rev. Lett. **76**, 1344 (1996).
[21] N. Bulut and D. J. Scalapino, Phys. Rev. B **47**, 3419 (1993).
[22] T. Dahm and L. Tewordt, Phys. Rev. Lett. **74**, 793 (1995).
[23] Y.-J. Kao, Q. Si, and K. Levin, Phys. Rev. B **61**, R11 898 (2000).
[24] M. R. Norman, Phys. Rev. B **75**, 184514 (2007).
[25] X. J. Zhou *et al.*, Nature (London) **423**, 398 (2003).
[26] S. A. Kivelson *et al.*, Rev. Mod. Phys. **75**, 1201 (2003).
[27] J. Zaanen, O. Y. Osman, H. V. Kruis, Z. Nussinov, and J. Tworzydło, Philos. Mag. B **81**, 1485 (2001).
[28] K. Machida, Physica (Amsterdam) **158C**, 192 (1989).
[29] K. Yamada *et al.*, Phys. Rev. B **57**, 6165 (1998).
[30] Y. J. Uemura, Solid State Commun. **120**, 347 (2001).
[31] H. H. Wen *et al.*, Europhys. Lett. **57**, 260 (2002).
[32] A. C. Fang *et al.*, Phys. Rev. Lett. **96**, 017007 (2006).
[33] R. Jamei, J. Robertson, E.-A. Kim, A. Fang, A. Kapitulnik, and S. A. Kivelson, Phys. Rev. B **74**, 174521 (2006).
[34] V. J. Emery, S. A. Kivelson, and O. Zachar, Phys. Rev. B **56**, 6120 (1997).
[35] S. A. Kivelson (private communication).